Experimental investigation and empirical correlations of heat transfer in different regimes of air-water two-phase flow in a horizontal tube

S.A. Nada
Department of Mechanical Engineering, Benha Faculty of Engineering, Banha University, Benha, Egypt
Tel.: +201066611381; fax: +20133230297
E-mail address: samehnadar@yahoo.com (Sameh Nada)

Abstract

The present article reports on experimental investigation of heat transfer to co-current air-water two phase flow in horizontal tube. The idea is to enhance heat transfer to the coolant liquid by air injection. Experiments were conducted for different air water ratios in constant temperature heated tube. Visual identification of flow regimes was supplemented. The effects of the liquid and gas superficial velocities and the flow regimes on the heat transfer coefficients were investigated. The results showed that the heat transfer coefficient generally increases with the increase of the injected air flow rate and the enhancement is more significant at low water flow rates. A maximum value of the two-phase heat transfer coefficient was observed at the transition to wavy-annular flow as the air superficial Reynolds number increases for a fixed water flow rate. It was noticed that the Nusselt number increased about three times due to the injection of air with at low water Reynolds. Correlations for heat transfer by air-water two phase flow were deduced in dimensionless form for the different flow regimes.

Keywords: *Heat transfer correlation; air-water two phase flow; flow regimes.*

NOMENCLATURE

C_p Specific heat of cooling water, kJ/kg K

D_i Tube inside diameter, m

D_o Tube outside diameter, m

h Average heat transfer coefficient, W/m^{2}K

h_L Single phase liquid heat transfer coefficient, W/m^{2}K

h_{TP} Tow phase average heat transfer coefficient, kJ/kg K

k Thermal conductivity, W/m K

L Tube length, m

$\dot{m}_c$ Mass flow rate, kg/s

Nu Average Nusselt number, dimensionless

Pr Prandtl number, dimensionless

q Heat transfer rate, W

Re Reynolds number, dimensionless

T Temperature, ˚C

U Superficial velocity, m/s

ΔT_{LM} Logarithmic mean temperature difference, ˚C

Subscripts

a Air

fd Fully developed

i Inlet flow to the test section

L Liquid single phase,

O Outlet flow from the test section

s,i Inner surface of the test section

TP Two phase

w Water

1. INTRODUCTION

Gas-liquid two-phase flow in tubes has a wide range of industrial and engineering applications such as chemical plants, nuclear reactors, oil wells, evaporators, condensers, solar power plants, etc. Also gas-liquid two- phase flow obtained by the injection of gas bubbles in a liquid can be used as a technique to enhance heat transfer to the flow [1, 2]. Gas-

liquid two- component two-phase flow pattern differs according to the gas and liquid flow rates. Numerous flow regime maps for adiabatic gas-liquid two-phase flow in horizontal pipes had been published from theory and experimental data over the past 50 years [3-7].

Investigation of the problems associated with heat transfer in single phase flow and in one-component two-phase flow during phase change process had received considerable attention due to its applications in heat exchange processes and during boiling and condensation process [8-11]. However, investigations of the problem associated with heat transfer in two- component gas-liquid two-phase flow in pipes had received less attention. Of the little investigations of heat transfer in two-component two-phase flow, the majority were developed from limited experimental data and only applicable to single flow pattern under constant heat flux boundary conditions [12]. Oshinowo et al. [13] developed two correlations for heat transfer coefficient in co-current vertical two-phase upflow and down flow of air-water under constant heat flux boundary conditions. Kim et al. [14] presented a new correlation to predict turbulent heat transfer coefficient for two-component two-phase flow in vertical pipes under constant heat flux boundary conditions. Heat transfer correlations in upward air-water two phase flow in inclined pipes for different flow regimes and for intermittent flow were developed under constant heat flux boundary conditions by Hetsroni et al. [15-16], respectively. Later, Kim and Ghajar [17] modified their previously developed robust two-phase heat transfer correlation for vertical pipe under constant heat flux boundary conditions [12] to predict the heat transfer coefficient for the horizontal pipe air-water two-phase flow under constant heat flux boundary conditions. Kaji et al. [18] carried out experimental measurements for heat transfer, pressure drop, and void fraction for upward heated air–water two-phase flow in 0.51 mm ID tube. To interpret the decrease of void fraction with decrease of tube diameter, a relation among the void

fraction, pressure gradient and tube diameter was derived. Heat transfer coefficient fairly agreed with the data for large diameter tube at relatively high air velocity but it became lower than that for larger diameter tubes at low air velocity. Vlasogiannis et al. [19] conducted experimental work and visual observations of air-water two phase flow as a cold stream in a plate heat exchanger. Flow regime map was constructed and the heat transfer coefficient of the air/water stream is measured as a function of air and water superficial velocities. Nilpueng, and Wongwises [20] studied air–water two-phase flow characteristics including flow pattern and pressure drop inside a plate heat exchanger with single pass under the condition of counter flow. The results showed that the annular-liquid bridge flow pattern appeared in both upward and downward flows. However, the bubbly flow pattern and the slug flow pattern are only found in upward flow and downward flow, respectively. The variation of the water and air velocity has a significant effect on the two-phase pressure drop.

As shown above, most of the two-component two-phase heat transfer studies were presented vertical tubes and under constant heat flux boundary conditions and only applicable to certain flow patterns, pipe orientation and fluid combinations. As it is well known, heat transfer rate, dimensionless parameters and correlations depends on the heat transfer boundary conditions. For the studied problems, such correlations are available in the literature for constant heat flux boundary conditions but are not available for constant temperature boundary conditions. To the author's knowledge, no experimental heat transfer data are available in the literature for air-water two-phase flow in horizontal pipes under constant temperature boundary conditions for the different possible flow patterns. Therefore the new in this work is to present experimental investigation for air-water two-phase flow in a horizontal pipe under constant temperature boundary conditions and develop heat transfers rates and correlations for the problem under constant temperature boundary conditions and at a wide range of air Reynolds number and two-phase flow regimes, which are not available in the literature. The studied problem can be encountered in many applications

such as steam condensers in the case of presence of some air with the cooling water. Also the idea can be used as a method of heat transfer augmentation by air injection.

2 Experimental Setup and Procedure

2.1 Experimental setup

A schematic diagram of the experimental setup is shown in Fig. 1. Water at ambient temperature, was circulated from a constant head tank (1) through the loop. The level of the tank was higher than the level of the test section by 10 m. The water flow rate was regulated by a valve (2) and was measured by a flow meter (3). The air was circulated through the loop by a compressor (4) through a receiver (5). The air pressure was regulated by a pressure regulator (6) and the air flow rate was regulated by a valve (8) and was measured by an orifice meter (7) with a digital pressure manometer across it. Two non return valves (9) were inserted in the air and water lines to prevent flow in the reverse direction. The air and water were mixed in a mixing chamber (10). The air water mixer consisted of a perforated copper tube inserted into the stream by means of a PVC T-section and a union section. The copper tube was connected with the T-section through the PVC union. Forty 1.6 mm holes positioned at 90° around the perimeter of the copper tube at 10 equally spaced axial locations along the length of the copper tube. Air-water mixer with the same idea was used previously by Ewing et al. [21] and Kim [22]. The air-water two phase stream leaving the mixer entered a transparent flow development section (11) which was a transparent acrylic tube of 24.5 mm I.D. It was used as a flow developing and turbulent reduction device and also as a flow pattern observation section. One end of the flow development section was connected with the gas liquid mixer through a PVC union and the other end was connected to the test section (12) through an acrylic flange. The test section was a

horizontal copper tube of 24.5 mm I.D. and 28.5 mm O.D. and L/Di =40. In order to apply constant temperature boundary conditions to the test section, the test tube was fitted in the center of 400 mm I.D. steel condenser shell (13). The test section was heated by saturated steam at atmospheric pressure, which was obtained from 27 kW, electric boiler (14). The steam was passed from the boiler to the condenser shell through l-in insulated steel pipe, condenses around the test section and the condensate from the condenser shell flowed through a steam trap (15) to a graduated collecting tank (16). The outlet air-water two-phase flow from the test section passed through another transparent acrylic tube (17) of 24.5 mm I.D. and L/di = 40. This transparent section was used as a flow pattern observation section. The air-water two phase outlet from this transparent section was connected to a gas-liquid separator (18). The mixer section, the two transparent flow pattern observation sections, and the test section were carefully leveled for reducing the effect of inclination on the flow pattern.

The temperatures of the test section were measured using 24 K-type thermocouple wires soldered on the outside wall of the test section at five equally spaced axial locations along the test section. The first axial location was at 100 mm from the entrance and the distance between each two axial locations was 200 mm. The axial location at the middle of the test section had 8 thermocouples positioned at 45° around the perimeter of the tube. Each of the other four thermocouple axial locations was containing 4 thermocouples positioned at 90° around the perimeter of the tube. Two other K-type thermocouples were used to measure the air-water mixture temperature at the entrance and the exit of the test section. To obtain the air-

water cup-mixed temperature at the exit of the test section a mixing well (19) was used. All the thermocouple wires were connected to a data acquisition system to record their readings aftersteady state condition was achieved. The readings of the thermocouples were averaged over a period of 60 second.

2.2 Experimental procedure

All the experiments were carried out at almost a uniform wall temperature, the difference between the tube wall surface temperatures at the exit and inlet of the test section was about 2-4°C depending on the flow rate inside the tube. After turning on the electric boiler and the air compressor, the required water flow rate was adjusted. Then the air flow rate was adjusted at small starting value. The air and water were mixed in the mixing chamber upstream of the test section. The air-water mixture passed through the test section. To heat the test section, the outlet steam from the boiler was allowed to pass through the condenser around the test section. The experiments were run at least one hour before steady state conditions were achieved, which was considered to be achieved when the measured tube wall temperatures were not changed by more than 0.5 °C within 10 minutes. When steady state conditions were established, the readings of all thermocouples, the water flow rate, pressure drop across the orifice air flow meter, the pressure of the air upstream the orifice meter, and the condensate flow rate were recorded. Also, the observations for flow pattern judgments were made at two locations: a location in the transparent section just before the test section and a location in the transparent section just after the test section. Keeping the water flow rate fixed, the air flow was readjusted to a new value to carry on a new experimental run and so on

until all the considered range of the air flow rate was covered. The water flow rate was then changed and the experimental procedure was repeated.

2.3 Experimental conditions

The experimental data were collected for the cases of single-phase water and the two-phase air-water heat transfer processes. The experiments for the single-phase water flow were carried out in the range of water Reynolds numbers $1780 \leq Re_w \leq 26600$. The experiments for air-water two-phase flow were carried out in the range of air superficial velocities $0.5 \leq U_a \leq 9$ m/s and water superficial velocities $0.04 \leq U_a \leq 0.42$ m/s. All the experiments were carried out using steam heated test section. The temperature of the steam used to heat the test section was the saturation temperature corresponding to the atmospheric pressure. Variation of the atmospheric pressure from standard atmospheric pressure was insignificant and the temperature of the saturated steam used for heating was taken 100 °C.

2.4 Data reduction

In order to calculate the heat transfer coefficients, the values of each of the temperatures and heat flux on the interior surface of the test section and the bulk temperatures of the fluid at inlet and exit of the test section were required. The rate of heat transfer, q, to the air-water two-phase flow across the test section was calculated by making heat balance between the air-water mixture water at inlet and exit of the test section as follows:

$$q = \dot{m}_w C_{pw}(T_o - T_i) + \dot{m}_a C_{pa}(T_o - T_i) = \dot{m}_w C_{pw}(T_o - T_i)(1 + \dot{m}_a C_{pa} / \dot{m}_w C_{pw}) \qquad (1)$$

Where $\dot{m}_w$ and $\dot{m}_a$ are the water and air flow rates in the two phase flow, respectively. T_o and T_i are the mixing cup two phase flow temperatures at the outlet and inlet of the test section. C_{pw} and

C_{pa} are the specific heat of the water and air, respectively. In Eqn.1, the order of magnitude of the term $(\dot{m}_a C_{pa} / \dot{m}_w C_{pw})$ in the studied ranges of parameters is about 0.0003 and this make that the effect of assuming the air and water temperatures equal the mixing cup temperatures in estimating the heat transfer rate in Eqn. 1 is very small and can be neglected. Moreover the flow mixing nature make the discrepancy in air and water temperature very limited which also vanishes any error in estimating the heat transfer by Eqn. 1

The average two phase heat transfer coefficient $\bar{h}_{TP}$ can be calculated from the relation

$$\bar{h}_{TP} = \frac{q}{\pi\ D_i\ L\ \Delta T_{LM}} \tag{2}$$

Where D_i and L are the inside diameter and the length of the test section; and ΔT_{LM} is the logarithmic mean temperature difference, which can be calculated from

$$\Delta T_{LM} = \frac{(\bar{T}_{s,i} - T_i) - (\bar{T}_{s,i} - To)}{\ln[(\bar{T}_{s,i} - T_i)/(\bar{T}_{s,i} - To)]} \tag{3}$$

Where $\bar{T}_{s,i}$ is the average inners surface temperature along the test section inner surface which was calculated from the measurements of the outside surface temperatures considering only one-dimensional heat conduction equation through the tube in the radial direction [8-11] from the equation,

$$T_{s,i} = T_{s,o} - \frac{q \ln(D_o / D_i)}{2\pi kL} \tag{4}$$

Where $\bar{T}_{s,o}$ is the average outer surface temperature along the test section, D_o is the outer diameter of the test section and k is the thermal conductivity of the test section material (copper). The average two phase Nusselt number $\overline{Nu}_{TP}$ based on the liquid properties can be calculated from

$$\overline{Nu}_{TP} = \frac{\bar{h}_{TP} D_i}{k_L} \tag{5}$$

Where k_L is the thermal conductivity of the water liquid.

2.5 Experimental uncertainties

The quantities measured directly included air and water flow rates, fluid bulk and tube surface temperatures and geometric dimensions. The air and water meters had an accuracy of ± 2%. All thermocouples were calibrated with accuracy of ± 0.1 °C; thus it was estimated that the uncertainty of the temperature difference was within ± 0.2 °C. The accuracy of the geometric dimensions were estimated to be ± 0.5%. Following the procedure of Holman Gajda [25], the uncertainties of the average Nusselt number and the Reynolds number during all the experiments were evaluated. It was estimated that the uncertainty in the average Nusselt number was within 7% and the uncertainty of the Reynolds number was within 3%.

2.6 Reliability and validation of the experimental set up

The overall reliability of the experimental set up and procedure was verified and validated by carrying out several experimental runs with only water (single phase) flowing inside the test section. The water Reynolds numbers of these experiments covered the laminar, transition, and turbulent flow regions of the heat transfer regimes. The single phase heat transfer data obtained from these experiments were compared and checked with the well known single phase heat transfer correlations [8-11]. These correlations of previous investigators were confirmed experimentally for fully developed region and for the range of conditions $0.7 \leq Pr \leq 160$ and $L/D \geq 10$ [8-11]. For long tube $L/D \geq 60$, it is reasonable to assume that the average Nusselt number Nu_L for the entire tube including the entry length is equal to the value associated with fully developed region ($Nu_{D,fd}$). However, for short tube $L/D \leq 60$ which is the case of the present work, Nu_L exceeds $Nu_{D,fd}$. Therefore $Nu_{D,fd}$ obtained from the equations of the previous investigations [8-11] for fully developed flow were corrected to take into consideration this effect using the equation

$Nu_L / Nu_{D,fd} = 1 + (L/D)^{2/3}$ [8-11]. Figure 2 shows the comparison of Nu_L of the present data for single phase with those obtained by previous investigators [8-11] after correction to include the entry length effect. The lower recommended Reynolds number range of Sieder and Tate and Dittus- Boelter's correlations is 10,000; while it was 2300 for Gnielinski's correlation [8-11]. Within the recommended range of Reynolds number of each correlation, the present data fall within a 5% deviation band of Gnielinski's correlation and 10% deviation band of Dittus-Boelter's and Sieder and Tate's correlations. These deviations are within the uncertainty errors (20% for Dittus- Boelter's and Sieder and Tate's correlations and 15% for Gnielinski's correlation. Therefore, the comparison showed that the presented data for single phase experiments agree well with those of previous investigators and this proofs the reliability and the validation of the experimental set up and the experimental procedure.

3. Results

3.1Flow regimes

The purpose of the identification of the flow pattern during the heat transfer experiments is to characterize the heat transfer process with the transition from one flow pattern to another. In this study the flow pattern identification was based on visual observations at two locations, just upstream and downstream the heat transfer test section. The experimental data were considered in the analysis when the observed flow patterns were the same at the two locations. The flow pattern observations were based under conditions when the superficial water velocity is kept constant and the superficial air velocity increases. For the ranges of superficial water and air velocities of the present heat transfer data, the flow pattern observed during the experiments were smooth stratified, wavy stratified, slug and annular wavy. In the observed stratified flow pattern, the water was flowing at the bottom of the pipe and the air

was flowing at the upper portion of the pipe. The water was separated from the air by either a smooth or wavy interface depending on the air flow rate. For small air flow rates the interface is smooth and the flow pattern was identified as smooth stratified flow. As the air flow rate increases, the velocity of the air increases and be sufficient to form waves on the interface, which becomes unstable and wavy. This flow pattern is identified as wavy stratified flow. As the water flow rate increases, the water level in the pipe becomes higher and the formed waves reached the top surface of the tube forming large slugs which filled the cross section of the tube. These slugs flow along the tube with the flow in an intermittent form. This flow pattern is identified as slug flow or intermittent flow. At high air flow rate and moderate water flow rate, water annulus with wavy air-water interface and water entrainment was observed. The water film at the bottom of the pipe was thicker than that at the top of the pipe. This flow pattern is identified as wavy annular flow.

The various flow patterns observed during the two-phase heat transfer experiments under the present test conditions are compared with the prediction of Taitels et al. [7] and Mandhane et al. [6] flow regime maps in Fig. 3, which are plotted in terms of the superficial air velocity U_a versus the superficial water velocity U_w . The figure shows that the transitions from smooth stratified flow to wavy stratified flow and from wavy stratified flow to wavy annular flow are reasonably predicted by the flow regime maps of Taitels et al. [7] and Mandhane et al. [6]. The air superficial velocity at which the transition from slug flow to annular-wavy flow occurs was predicted fair enough by Taitels et al. map [7] and over predicted by Mandehan et al. map [6]. Both of Taitels et al. and Mandehan et al. maps tend to slightly under predict the liquid superficial velocity at which the transition from stratified wavy flow to slug or annular-wavy flows occurs.

3.2 Air-water two-phase heat transfer data

The results obtained for the two-phase heat transfer data are shown in Fig. 4. Two-phase Nusselt number based on the liquid properties, has been plotted against air Reynolds number Re_a for the six investigated water Reynolds numbers. It can be seen from Fig. 4 that, the Nusselt number generally increases as the air Reynolds number increases for a fixed water Reynolds number. This can be attributed to the increase of the water and mixture velocities due to the addition of the air phase. The increase of the water and mixture velocities increases the turbulence level and the mixing action of the air-water two-phase flow. The increase of the mixing action and the turbulence level decrease the thermal resistance to heat transfer and consequently increases the heat transfer coefficient. The increase of the heat transfer coefficient with the increase of the air Reynolds number was also observed by previous investigators [22] for gas-liquid two-phase flow in horizontal pipes under constant heat flux boundary conditions. Also, Fig. 4 shows that at lower water Reynolds number where stratified flow regimes exist, the increase of the Nusselt number with the increase of the air Reynolds number was gentle. While for high water Reynolds number where intermittent flow regimes exist, the increase of the Nusselt number with the increase of the Reynolds number was not gentle. This can be attributed to the nature of the intermittent flow regimes where pulses of air- water clusters exist and increase with the increase of the liquid and gas flow rates and this makes the increase of the Nusselt number is not a gentle one. Also Fig. 4 shows that for higher water flow rates $Re_w \geq 6400$ there exist a maximum value of Nu_{TP} as Re_a increases for a fixed water flow rate, i.e., for higher water flow rates, the two phase Nusselt number increases with the increase of the injected air flow rate and then it decreases. The decrease of the two-phase Nusselt number may be attributed to the liquid entrainment occurred at high air flow rates. As shown in Fig. 4, the maximum value of Nu_{TP} occurs in the range of $5600 < Rea < 7400$ (i.e. $3.5 < Ua < 4.5$ m/s) for $Re_w > 6397$ (i.e.

U_w > 0.166 m/s). As shown in Fig. 3, this region is the transition region to wavy annular flow. The decrease of the two-phase Nusselt number due liquid entrainment and transition to wavy annular with the increase of air flow rate can be attributed to the less liquid contact with the heat transfer surface in this regions. The existence of a maximum value of Nu_{TP} was also observed by previous investigations [17, 22] for air-water two-phase flow in vertical and horizontal pipes at constant heat flux.

Figure 5 shows the variation of the ratios of Nusselt number of two-phase flow to those obtained in single-phase water flow versus the air Reynolds umber for the different water Reynolds numbers. As shown in the figure, the percentage increase of the Nusselt number due to the increase of the air flow rate at low water flow rates is higher than that at high water flow rates. For example at water Reynolds number equals to 1780, the Nusselt number increased about three times due to the injection of air with Re_a =14000 (i.e. U_a = 8 m/s), while at water Reynolds number equals to 15343, the Nusselt number increased about two times due to the injection of air with the same Reynolds number. This means that, the increase of the two-phase Nusselt number with the increase of the air Reynolds number was more significant at low water flow rates than that at high water flow rates. This can be attributed to the following: at low water low rates, the flow is laminar or turbulent with small turbulence level in the water stream before the injection of the air stream. The injection of the air stream into the water stream increases the turbulence level. At high water flow rate, the flow is turbulent and the turbulence level is already high before the injection of the air stream. This means that the percentage increase of the turbulence level due to the injection of the air stream in the case of low water low rate is higher than that in the case of high water flow rate. This makes the percentage increase of the Nusselt number due to the injection of the air stream in the case of low water flow rate higher than that in the case of high water flow rate. The same results were observed for two-

phase flow in a vertical pipe by Groothuis and Hendal [23] and Zaidi and Sims [24] and and for a horizontal pipe at a constant heat flux by Kim [22]. These investigators found that the influence of the air on heat transfer was most pronounced at the lowest liquid Reynolds number.

3.3. Experimental correlations

From the test results, it was found that the heat transfer behavior is different for the different ranges of superficial water and air Reynolds numbers. The results shown in Figs. 4 and 5 indicate that three different ranges of superficial water and air Reynolds numbers have three different behaviors of the average two-phase Nusselt number curves. The following correlations were obtained for these different ranges of superficial water and air Reynolds number:

1. For $0 \leq Rew \leq 3500$ and $0 \leq Rea \leq 15500$

$$\overline{Nu}_{TP} / \overline{Nu}_{L} = 1 - 5 \times 10^{-4} \, \mathrm{Re}_{w}^{-1} (3.8 \times 10^{-5} \, \mathrm{Re}_{a}^{2} - \mathrm{Re}_{a}) \qquad (6)$$

The flow regime corresponding to these ranges of Re_w and Re_a is stratified flow shown in Fig. 3. The comparison of the prediction of this correlation with the 20 stratified flow experimental data points of the current study is shown in Fig. 6-a. As shown in this figure, the recommended correlation (Eq. 6) predicts the two-phase heat transfer coefficient quite well. The prediction was within ±10% for all the data points and was within ± 5% for 92% of the data points.

2. For $7000 \leq Re_w \leq 17800$ and $0 \leq Re_a \leq 7000$

$$\overline{Nu}_{TP} / \overline{Nu}_{L} = 1 - 0.2314 \mathrm{Re}_{w}^{-0.77} (10^{-5} \, \mathrm{Re}_{a}^{2} - \mathrm{Re}_{a}) \qquad (7)$$

The flow regime corresponding to these ranges of Re_w and Re_a is intermittent flow as shown in Fig. 3. The comparison of the prediction of this correlation with the 23 intermittent flow experimental data points of the current study is shown in Fig. 6-b. As shown in this figure, the recommended correlation (Eq.7) predicts the two-phase heat transfer coefficient quite

well. The prediction was within ±15% for all the data points and was within ±10% for 90% of the data points.

3. For $7000 \leq Re_w \leq 17800$ and $8000 \leq Re_a \leq 15500$

$$\overline{Nu}_{TP} / \overline{Nu}_L = 1 + 145 Re_w^{-0.415} Re_a^{-0.116} \quad (8)$$

The flow regime corresponding to these ranges of Re_w and Re_a is wavy annular flow as shown in Fig. 3. The comparison of the prediction of this correlation with the 17 wavy annular flow experimental data points of the current study is shown in Fig. 6-c. As shown in his figure, the recommended correlation (Eq. 8) predicts the two-phase heat transfer coefficient quite well. The prediction is within ± 5% for all the data points.

The single liquid phase Nusselt number Nu_L in Eqns. 6-8 can be calculated from the well-known single phase heat transfer correlations of previous investigators [8]. All properties appearing in Eq. 6-8 were evaluated at the average value of the bulk temperatures at the inlet and exit of the test section $(T_{wi} + T_{wo})/2$.

4. Conclusions

The heat transfer of air-water two-phase flow in a tube under constant temperature has been experimentally investigated in the present study for different flow patterns: stratified, slug and wavy-annular flows. In order to achieve this investigation a two-phase heat transfer experimental setup was built and validated with experimental data for single phase heat transfer. The results of comparing the single phase heat transfer data with previous correlations and the results of comparing the observed flow patterns with the previous flow regime maps indicated that both of them agreed quite well with each other. The air-water two-phase heat transfer data showed that the heat transfer coefficients generally increase as the air superficial Reynolds number increases for a fixed water flow rate. However, a maximum value of the two-phase heat transfer coefficient was observed as the air

superficial Reynolds number increases for a fixed water flow rate. This maximum value was observed at the transition to wavy-annular flow. Three correlations for three different ranges of water and air flow rates were derived from the experimental data to predict the heat transfer coefficient for air-water two-phase flow in a steam heated horizontal tube which is usually considered as constant temperature heat transfer process. The correlations predicted the present experimental data with a maximum deviation of ± 15% .

REFERENCES

1. D.B.R. Kenning, Y.S. Kao, Convective heat transfer to water containing bubbles: enhancement not dependent on thermo capillary, International Journal of heat mass transfer, 15 (1972) 1709-1718.
2. M. Tamari, K. Nishikawa, The stirring effect of bubbles upon heat transfer to liquids. Heat transfer-Japanese Journal, 5 (1976) 31-44.
3. D. Barnea, Y. Luninski, Y. Taitel, Flow pattern in horizontal and vertical two phase flow in small diameters pipes, Can. J. Chern. Eng., 61 (1983) 617-620.
4. D. Barnea, O. Shoham, Y. Taital, Y., A.I Dukler, Flow pattern transition for horizontal and inclined pipes: Experimental and comparison with theory, Int. J. Multiphase Flow, 6 (1980) 217-225.
5. K. J. Bell, J. Taborek, F. and Fenoglio, Interpretation of horizontal in tube condensation heat transfer correlations with a two-phase flow regime map, Chern. Eng. Prog. Symp. Ser., Vol. 66 No. 102 (1970) 150-163.
6. J.M andhane, G.A. Gregory, K. Aziz, A flow pattern map for gas liquid flow in horizontal pipes, Int. J. Multiphase Flow, 1 (1974) 537-553.
7. Y. Taitel, A.E. Dukler, A model for predicting flow regime transitions in horizontal and near horizontals gas-liquid flow, AICHE J., 22 (1976) 47-54.

8. V. Gnielinski, Forced convection in ducts. In handbook of heat exchanger design, ed. Hewitt, G.F. New York: Hemisphere Publishing, 1990.
9. Incropera, F.P., and Witt, D.P., Introduction to heat transfer, Chapter 8, New York: Wiley Publishing, 2000.
10. Rohsenow, W.M., Boiling. In handbook of heat transfer fundamentals. Eds. Rohsenow, W.M., Harnett, J.P., and Ganic, E.N. New York: McGraw-Hill, 1985.
11. Suryanarayana, N.V., Engineering Heat Transfer, chapter 4, New York: West Publishing Company, 1995.
12. D. Kim, A.J. Ghajar, R.L Dougherty, Developed of improved two phase two-components pipe flow heat transfer correlations from existing correlations and published data, 5th ASME/JSME Joint thermal engineering conference, San Diego, CA, Paper No. AJTE-99-6122, March 15-19, 1999.
13. T. Oshinowo, R.C. Betts, M.E Charless, Heat transfer in co-current vertical two-phase flow, The Canadian Journal of Chemical Engineering, 62 (1984) 194-198.
14. D. Kim, A.J. Ghajar, R.L. Dougherty, Robust heat transfer correlation for turbulent gas-liquid flow in vertical pipes, J. Thermophys. Heat Transfer, 14 (2000) 574-578.
15. G. Hetsroni, J.H. Yi, B.G. Hu, A. Mosyak, L.P. Yarin, G. Ziskind, Heat transfer in intermittent air-water flows - Part II - Upward inclined tube, Int. J. Multiphase Flow, 24 (1998) 189-212.
16. G. Hestroni, D. Mewes, C. Enke, M. Gurevich, A. Mosyak, R. Rozenblit, heat transfer in two phase flow in inclined tubes, Int, J. Multiphase Flow, 29 (2003) 173-194.
17. D. Kim, A.J. Ghajar, Heat transfer measurements and correlations for air-water flow of different flow patterns in a horizontal pipe, Experimental Thermal and Fluid Science, 25 (2002) 659-676.

18. M. Kaji, T. Sawai, Y. Kagi, T. Ueda, Heat transfer and fluid dynamics of air–water two-phase flow in micro-channels, Experimental Thermal and Fluid Science, 34 (2010) 446–453.
19. P Vlasogiannis, G Karagiannis, P Argyropoulos, V Bontozoglou, Air–water two-phase flow and heat transfer in a plate heat exchanger, International Journal of Multiphase Flow, 28 (2002) 757–772.
20. k. Nilpueng, S. Wongwises, Two-phase gas–liquid flow characteristics inside a plate heat exchanger, Experimental Thermal and Fluid Science, 34 (2010) 1217–1229.
21. M.E Ewing, J.J Weinandy, R.N. Christensen, Observations of two-phase flow patterns in a horizontal circular channel, Heat Transfer Eng. 20 (1999) 9-14.
22. D. Kim, Heat transfer correlations for air-water two-phase flow of different flow patterns in a horizontal pipe, KSME International Journal, 15 (12) (2002), 1711–1727
23. H. Groothuis, W.P. Hendal, Heat transfer in two phase flow, Chem. Eng. Sci., 11 (1959) 212-220.
24. A.J. Zaidi, G.E. Sime, The effect of a surfactant on flow patterns, pressure drop and heat transfer in two-phase two-components vertical flow, in: C.L. Tien, V.P. Carey, J.K. Ferrell (EDS.), presented at the 8 th International heat transfer conference, San Francisco, CA, 5, (1986) 2283-2288.
25. J.P. Holman, and W.J. Gajda, Experimental method for engineering, McGraw Hill, New York, 1989.

Figures captions

Fig. 1. Schematic of Experimental set up

Fig. 2. Comparison of present water single phase data with previous correlations

Fig.4. Variation of $\overline{Nu}_{TP}$ versus superficial air velocity

Fig.3. Comparison of the present flow pattern with previous flow regime maps

Fig. 5. Variation of $\overline{Nu}_{TP} / \overline{Nu}_{L}$ versus superficial air velocity

Fig. 6. Comparison between experimental data and correlations predictions

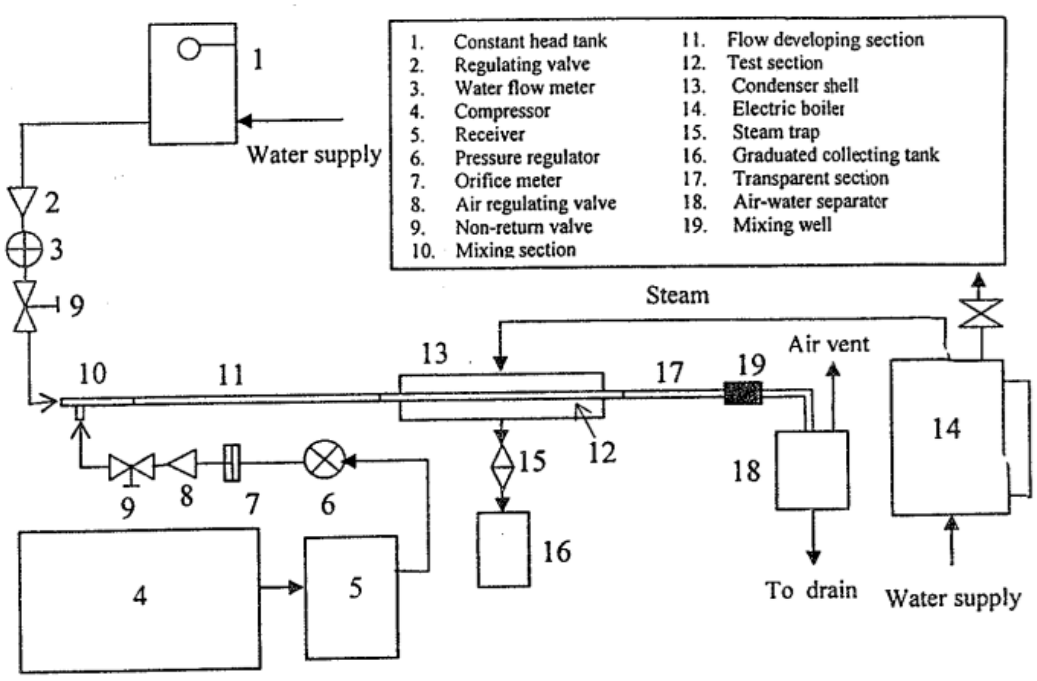

Fig. 1. Schematic of Experimental set up

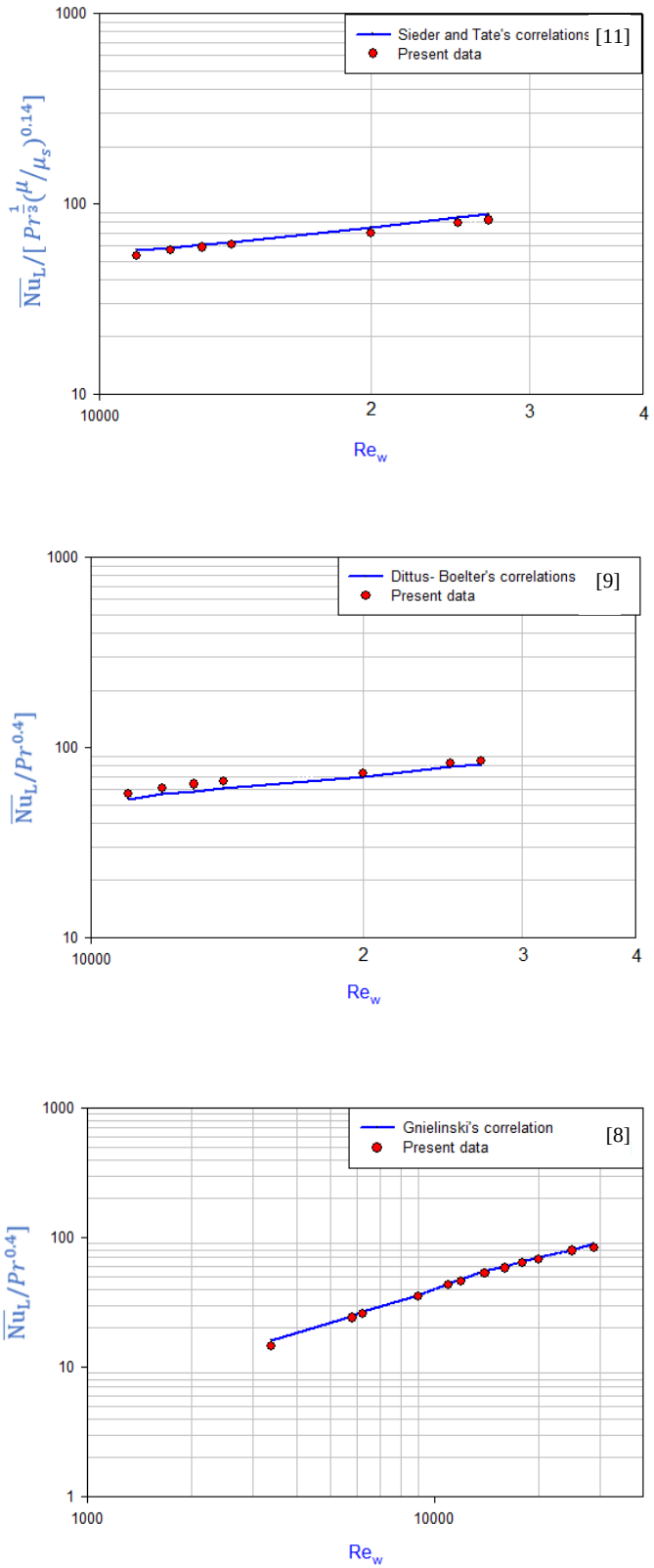

Fig. 2. Comparison of present water single phase data with previous correlations

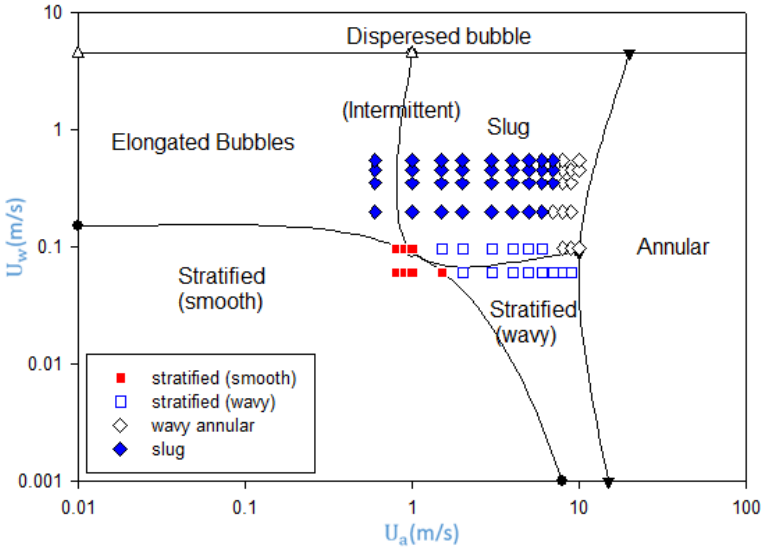

(a) Comparison with Mandhan et al. [6] map

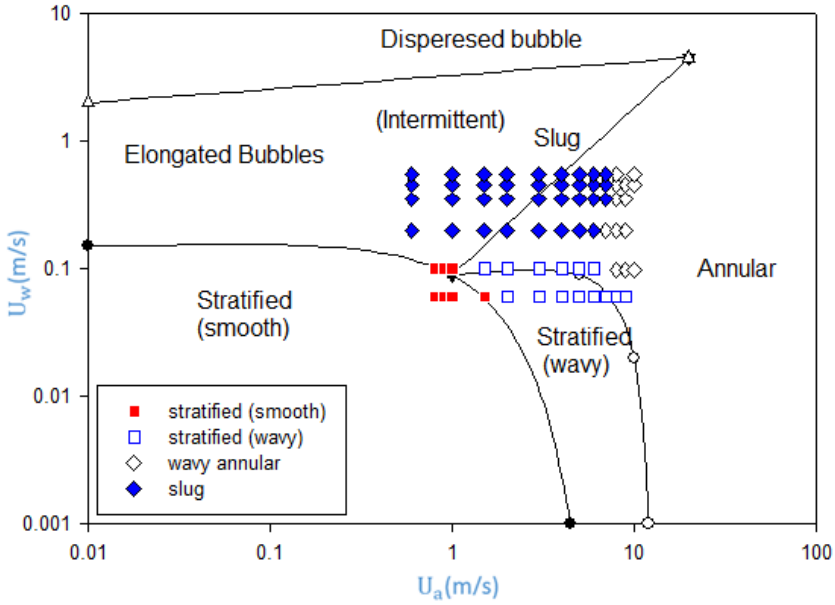

(b) Comparison with Taitels et al. [7] map

Fig.3. Comparison of the present flow pattern with previous flow regime maps

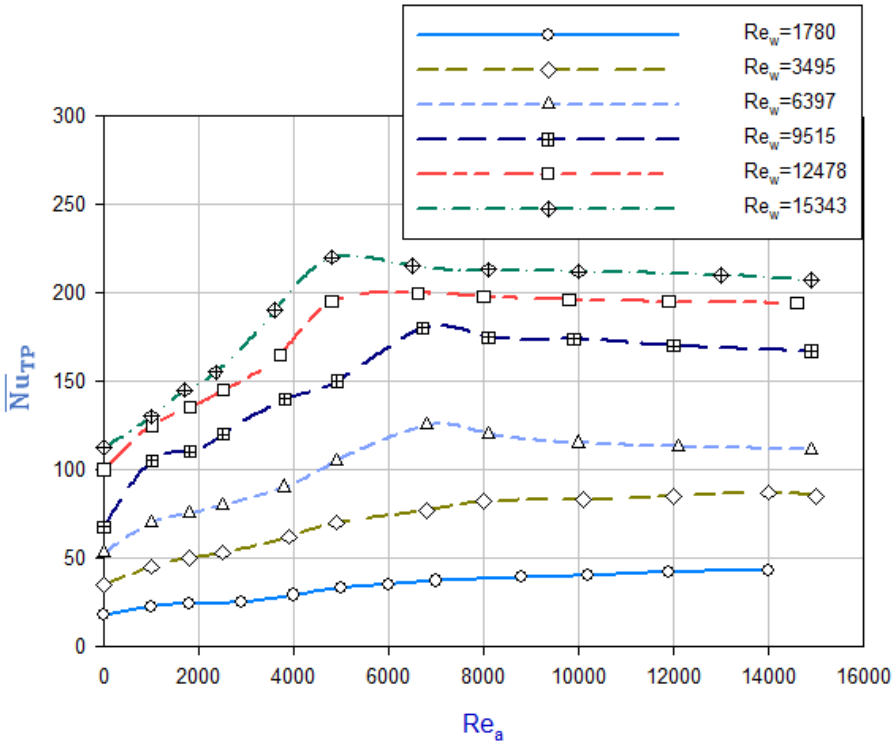

Fig.4. Variation of $\overline{Nu}_{TP}$ versus superficial air velocity

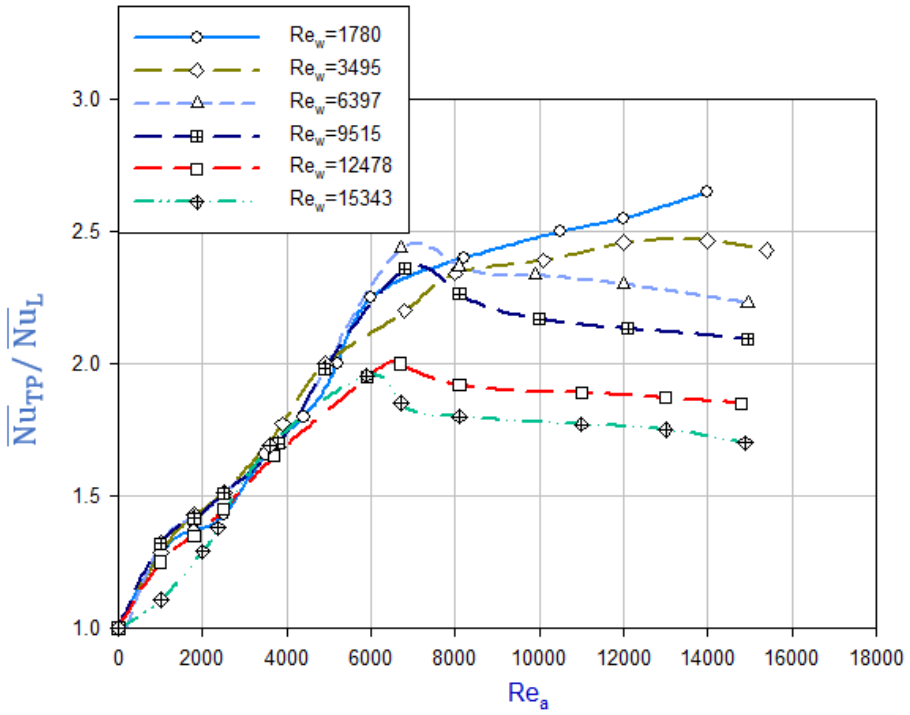

Fig. 5. Variation of $\overline{Nu}_{TP} / \overline{Nu}_{L}$ versus superficial air velocity

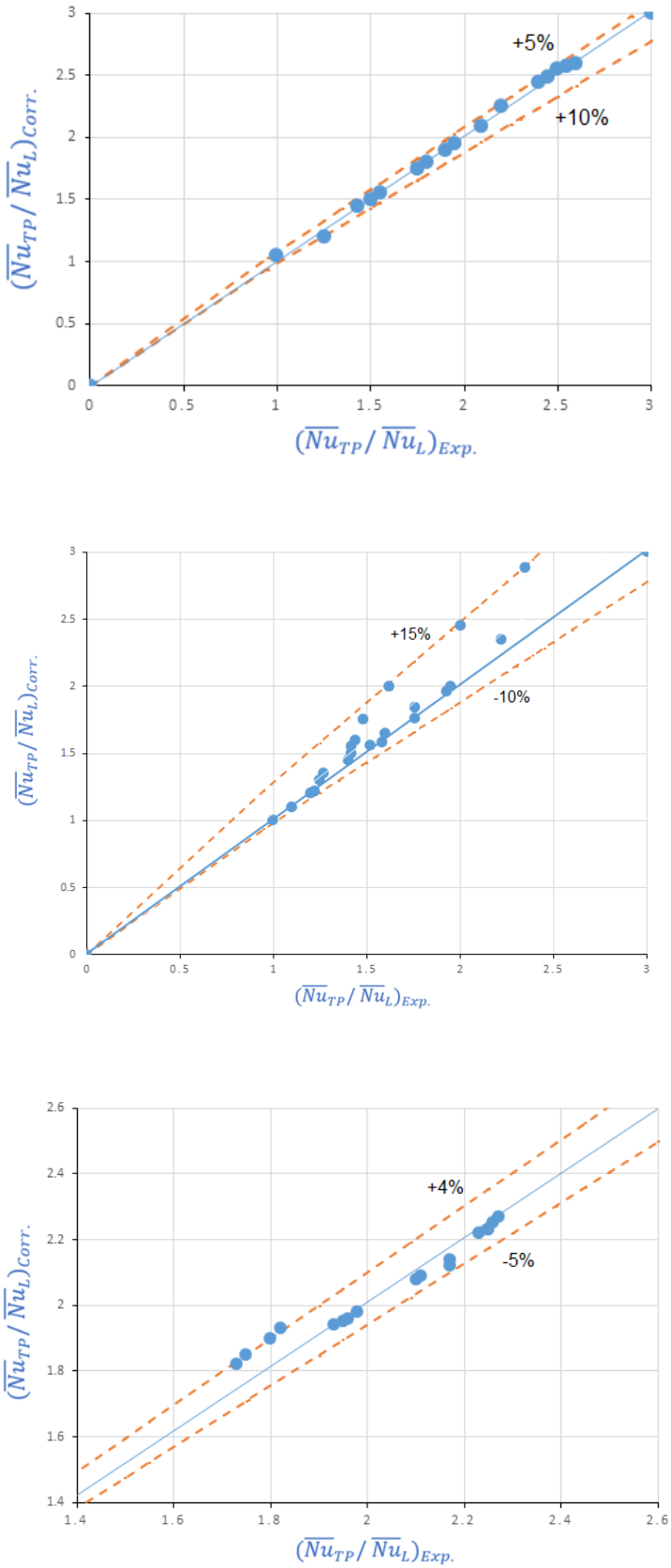

Fig. 6. Comparison between experimental data and correlations predictions